Observation of Large-Transverse-Momentum Muons Directly Produced by 300-GeV Protons*

J. P. Boymond, R. Mermod,† P. A. Piroué, and R. L. Sumner
Department of Physics, Joseph Henry Laboratories, Princeton University, Princeton, New Jersey 08540
and
J. W. Cronin, H. J. Frisch, and M. J. Shochet
The Enrico Fermi Institute, University of Chicago, Chicago, Illinois 60637
(Received 8 May 1974)

We have observed muons produced directly in Cu and W targets by 300-GeV incident protons. We find a yield of muons which is approximately a constant fraction (0.8×10^{-4}) of the pion yield for both positive and negative charges and for transverse momenta between 1.5 and 5.4 GeV/c.

In this Letter we report on the observation of muons produced directly in nuclear targets by 300-GeV incident protons. Study of muon production at high transverse momentum was originally motivated by the search for the intermediate vector boson. Early experiments were carried out at the Argonne zero-gradient synchrotron[1] and the Brookhaven alternating-gradient synchrotron[2] with negative results. More recently, several experiments have shown evidence for the direct production either of single muons[3,4] or of muon pairs[5] in nucleon-nucleon collisions. Extensive theoretical work[6,7] suggests that collisions of pointlike constituents of the nucleon would result in the direct production of muons.

In this experiment, performed at the National Accelerator Laboratory (NAL), we have used an apparatus described in a previous publication.[8] It consists of a single-arm focusing spectrometer equipped with two Cherenkov counters and a calorimeter to identify hadrons, and a 15-ft-long steel filter sampled each 2.5 ft with dE/dx counters to identify muons. The spectrometer viewed secondaries produced in a heavy target at an angle of 77 mrad relative to the incident 300-GeV proton beam. This angle corresponds to ~90° in the nucleon-nucleon c.m. system. Direct muons from the target were separated from muons coming from π and K decays in flight with the aid of two absorbers which could be inserted into the spectrometer close to the target. The first absorber was a 23-in.-long W block with its upstream face 9.5 in. from the center of the target. The second absorber was a 42-in.-long Fe block with its upstream face 42 in. from the target. We used a 2-in.-long W target, primarily in runs with negative muons, and a 3-in.-long Cu target primarily in runs with positive muons.

Data were taken under three conditions: (1) no absorber, (2) W absorber inserted only, and (3) Fe absorber inserted only. Runs were made at 10-GeV/c intervals between 20 and 70 GeV/c corresponding to transverse momenta ($P_\perp$) from 1.5 to 5.4 GeV/c. At 20 and 30 GeV/c, data were also taken with both absorbers in the beam as a consistency check. To verify that the muons were associated with the target, we also took data with the target removed for the three principal conditions at 20, 30, and 40 GeV/c.

For each absorber condition we measured the ratio of muons detected at the end of our apparatus to pions of the same charge detected by the apparatus when the absorber was absent. Two counter telescopes which looked at the target at 90° laboratory angle permitted normalization of different runs. The yield of pions with no absorber was corrected for nuclear absorption in the remainder of the apparatus and for decay in flight.

The hadrons were attenuated by factors of ~200 and ~270 with the W and Fe absorbers, respectively. These rather small attenuations resulted in a significant hadron penetration. These hadrons were identified by the combination of the Cherenkov counters and the hadron calorimeter. Those decaying appeared as muons. Thus the observed muons with absorber in place consisted of three components: (1) muons produced directly in the target, (2) muons produced by hadrons decaying upstream of the absorber, and (3) decay muons from hadrons which penetrated the absorber.

For process (3) the ratio of muons to pions[9] was directly measured at each momentum and polarity in runs without the absorbers; the corresponding muon yield in the absorber runs is calculated from the observed penetrating pions. The remaining muon yield coming from process-

TABLE I. Reduction of raw data to direct muon yield at the target. Processes (1), (2), and (3) are referred to in the text. "Tungsten" and "Iron" refer to the particular absorber used.

	Tungsten	Iron
Observed muons	795 ± 28	623 ± 25
Observed pions	13 580	4985
Ratio μ/π without absorber	$(2.03 \pm 0.10) \times 10^{-2}$	
Muons from hadron penetration of absorber, process (3)	276 ± 13	101 ± 5
Muons from processes (1) and (2)	519 ± 31	522 ± 26
Absorber loss factor	0.71 ± 0.04	0.40 ± 0.02
Corrected muons from processes (1) and (2)	731 ± 60	1305 ± 92
Pions at target	4.60×10^6	4.62×10^6
Muons/pions at target	$(1.59 \pm 0.13) \times 10^{-4}$	$(2.83 \pm 0.20) \times 10^{-4}$
Effective distance to target (m)	0.35	1.25
Extrapolated μ/π at target	$(1.10 \pm 0.15) \times 10^{-4}$	

es (1) and (2) is then corrected for the loss due to the absorber insertion (e.g., multiple scattering). Finally, the direct muon yield is obtained by linear extrapolation to zero decay path.

In Table I we present the reduction of the raw data from a typical run at 40 GeV/c. The absorber loss factors, calculated by Monte Carlo techniques, are presented in Table II. These factors account for the multiple-scattering loss, as well as the increased yield due to acceptance of smaller $P_\perp$ when the absorber is in place. The dependence of yield on $P_\perp$ was taken from our previous measurements of hadron production.[8] We thus assume that the direct muon component has a similar dependence on $P_\perp$, an assumption that can be checked *a posteriori*. Figure 1 shows the corrected results of a typical run along with the *predicted* slope. The points are plotted at a distance $d+\lambda$, where d is the distance between the target and the upstream end of the absorber and λ is the measured interaction length in the absorber.

The predicted slope can be obtained from the rate of hadron decay between the target and the absorber. It was calculated by numerical integration as a function of momentum. The yield of decay muons between the target and absorber depends on both K and π decays. Kaons are twice

TABLE II. Calculated absorber loss factors.

Momentum (GeV/c)	Tungsten	Iron
20	0.42 ± 0.03	0.182 ± 0.015
30	0.56 ± 0.03	0.300 ± 0.015
40	0.71 ± 0.04	0.40 ± 0.02
50	0.81 ± 0.05	0.47 ± 0.02
60	0.87 ± 0.04	0.54 ± 0.02
70	1.02 ± 0.04	0.62 ± 0.03

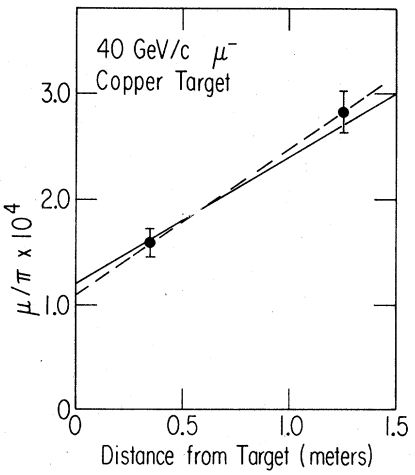

FIG. 1. Plot of data reduced in Table I. Dashed curve, linear extrapolation to the target; solid line, calculated slope.

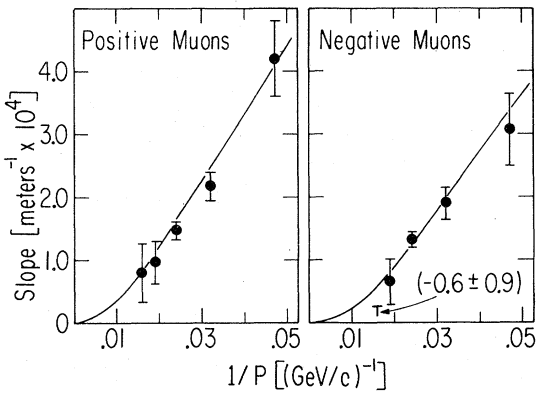

FIG. 2. Plot of observed slope and calculated slope versus reciprocal of the muon momentum. Points, experimentally measured slopes; solid line, calculated slope. The slope as a function of $1/P$ is expected to be a parabola. The decrease in the K/π ratio towards low momentum distorts the parabolic shape.

as effective as pions in producing detected muons. Thus the slope is sensitive to the K/π ratio at the target. Figure 2 shows for both charges the predicted and observed slopes plotted against the inverse of the muon momentum.

The agreement between calculated and observed slopes is a significant verification of the corrections which are quite different in nature for the two absorbers. The W absorber is more sensitive to the broadening of the acceptance because of its proximity to the target, but is less sensitive to multiple scattering for the same reason. The inverse is true for the Fe absorber.

Table III gives the ratio of direct muons to pions at the target for all conditions. The most striking aspect of these results is the constancy of the ratio μ/π. The constancy for different target materials is particularly interesting. In a separate experiment, to be reported in a subsequent publication, we have found the yield of pions per interacting proton at 3-GeV/c $P_\perp$ to be 3.5 times larger from a W target than a Be target. This effect is believed to be due to secondary scattering in the nucleus. Since the direct muons follow the same pattern, a strongly interacting, short-lifetime source is suggested for the muons.

One such source can be the known vector mesons. For example, if ρ and φ were each produced with the same cross section as π, we would expect a ratio $(\mu/\pi)\times 10^4$ of 0.68, 0.46, and 0.33 at $P_\perp$ of 1.5, 3.0, and 4.5 GeV/c, respectively.

In Figure 3 we plot the invariant cross section

TABLE III. Ratio of directly produced muons to pions in the proton-nucleus collision. The number of observed pions emerging from the 0.4-interaction-length target is multiplied by a factor 1.25 to account for absorption in the target itself.

$P_\perp$ (GeV/c)	$10^4\times\mu/\pi$ (target) Positive	Negative
1.62	0.66 ± 0.25 (Cu)	0.86 ± 0.20 (W)
2.38	0.72 ± 0.11 (Cu)	0.67 ± 0.12 (W)
3.15	0.88 ± 0.18 (Be)	...
3.15	0.94 ± 0.16 (Cu)	0.88 ± 0.12 (Cu)
3.15	0.60 ± 0.15 (W)	0.74 ± 0.16 (W)
3.91	0.98 ± 0.23 (Cu)	0.88 ± 0.26 (W)
4.67	0.87 ± 0.30 (Cu)	1.02 ± 0.34 (W)
5.44	0.94 ± 0.47 (Cu)	1.20 ± 0.46 (W)

per nucleon for inclusive muon production. Also plotted is the inclusive pion cross section multiplied by 10^{-4} and the inclusive muon cross section expected from a model based on parton-antiparton annihilation.[10] It is clear that the yield of muons is everywhere in excess of the parton-model prediction.[11]

We wish to thank the staff of the Proton Section

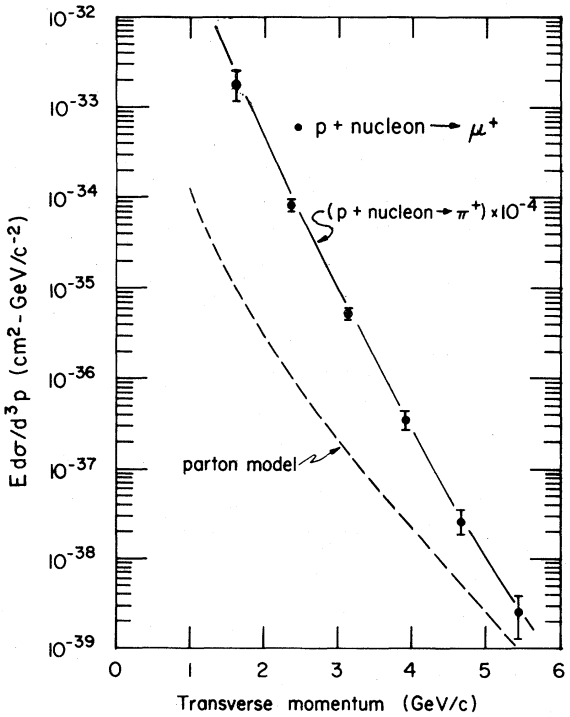

FIG. 3. Plot of the invariant cross section for direct muon production versus P. Also shown is the pion cross section multiplied by 10^{-4} and the cross section predicted by a parton model.

of NAL for their magnificent support of this experiment. We also wish to thank V. L. Fitch, S. B. Treiman, E. A. Paschos, and G. R. Farrar for valuable discussions. Finally, one of us (R.M.) wishes to thank NAL for its hospitality and support.

*Work supported by the National Science Foundation and the U. S. Atomic Energy Commission.

†On leave at NAL from the University of Geneva, Geneva, Switzerland.

[1]R. C. Lamb *et al.*, Phys. Rev. Lett. 15, 800 (1965).

[2]R. Burns *et al.*, Phys. Rev. Lett. 15, 830 (1965).

[3]P. J. Wanderer *et al.*, Phys. Rev. Lett. 23, 729 (1969).

[4]G. B. Bondarenko *et al.*, as cited by V. Lebedev in *Proceedings of the Sixteenth International Conference on High Energy Physics, The University of Chicago and National Accelerator Laboratory, 1972,* edited by J. D. Jackson and A. Roberts (National Accelerator Laboratory, Batavia, Ill., 1973), Vol. 2, p. 329.

[5]J. Christenson *et al.*, Phys. Rev. Lett. 25, 1523 1523 (1970).

[6]S. D. Drell and T. M. Yan, Phys. Rev. Lett. 25, 316 (1970).

[7]J. D. Bjorken, J. Phys. (Paris), Colloq. 34, C1-385 (1973).

[8]J. W. Cronin *et al.*, Phys. Rev. Lett. 31, 1426 (1973).

[9]For convenience we normalize to pions; the pions serve as a measure of all hadrons.

[10]G. R. Farrar, to be published.

[11]The yield of muons from the parton-antiparton annihilation process depends critically on the assumed antiparton distributions in the nucleon. The constraints on these distributions from inelastic electron and neutrino scattering make it unlikely that a parton model can account for the large observed muon yields.

Anomalous Muon and Hadron Charge Ratios in Secondary Cosmic Rays

Robert K. Adair
Yale University, New Haven, Connecticut 06520
(Received 18 March 1974)

Secondary cosmic-ray muon and hadron fluxes are calculated for particle energies above 200 GeV using accelerator data on inclusive hadron cross sections and the known primary flux. The gross differences between the calculated and measured muon and hadron charge ratios require radical reexamination of conventional views on hadron interactions or the neutron-proton ratio in the primary flux.

It is clearly possible to derive the characteristics of secondary cosmic-ray fluxes knowing the composition of the primary flux and the details of hadron-hadron interactions. In the energy region of 1000 GeV per nucleon, the primary flux intensity can be described by the relation[1,2]

$$dN/dE = A(\gamma - 1)E^{-\gamma}, \quad (1)$$

where $A = 1.5 \pm 0.25$ cm^{-2} sec^{-1} sr^{-1}, $\gamma = 2.72 \pm 0.05$, and E, the energy per nucleon, is measured in GeV. Measurements of the charge spectrum[2] of the primaries at energy extending up to 400 GeV per nucleon indicate that about 89% of the nucleon flux are protons and 11% neutrons assuming that charge-1 particles are protons and charge-2 particles are α particles. Only hadron-hadron inclusive cross sections are necessary for an understanding of inclusive secondary fluxes; and proton-proton inclusive cross sections have been measured[3] up to laboratory energies of 1500 GeV at the CERN intersecting storage ring (ISR) facility, and meson interactions have been studied in accelerator experiments at lower energies. From this knowledge of the primary flux and the hadron interaction inclusive cross sections and the use of conventional assumptions concerning charge independence and factorization in the hadron-hadron fragmentation region, one can calculate secondary cosmic-ray fluxes precisely, in principle, if one neglects correlation effects or coherent effects in the projectile or target. Since these effects are not likely to be large, plausible estimates of these nuclear effects allow reliable calculations of the secondary fluxes. Although there is a long history of such calculations,[4] and the results presented here differ from many, but not all, of the previous conclusions, only now do we have sufficiently extensive and reliable data on the basic hadron interactions so that complete calculations can be made which are sufficiently accurate so that differences between the results of the calculations and measurements can confidently be ascribed to inadequacies in the conventional assumptions used